Available online at www.sciencedirect.com
ScienceDirect
Journal of Power Sources 165 (2007) 609–615
JOURNAL OF POWER SOURCES
www.elsevier.com/locate/jpowsour

New manganese dioxides for lithium batteries

W. Bowden [a,*], T. Bofinger [a], F. Zhang [a], N. Iltchev [a], R. Sirotina [a], Y. Paik [b], H. Chen [b], C. Grey [b], S. Hackney [c]

[a] *Gillette Technology Center, US, Needham, MA 02492, United States*
[b] *Stony Brook University, Stony Brook, NY 11794, United States*
[c] *Michigan Technical University, Houghton, MI 49931, United States*

Available online 13 November 2006

Abstract

Lithium/manganese dioxide primary batteries use heat treated manganese dioxide (HEMD), a defect pyrolusite structure material as the cathode active material. Ion exchange of the structural protons in electrolytic manganese dioxide (EMD) with lithium before heating results in formation of a lithium containing γ-MnO_2. Increased lithium hydroxide concentration and increased temperature lead to increased lithium levels. At 80 °C with a combination of LiOH and LiBr, almost all of the structural protons in MnO_2 are replaced by lithium resulting in a γ-MnO_2 phase substantially free of protons and containing about 1.8% Li. This highly substituted lithium containing MnO_2 is reduced at between 3.5 and 1.8 V and has a capacity of 250 mAh g^{-1}. There are two reduction processes, one at 3.25 and the other at 2.9 V. TGA studies reveal two processes during heat treatment. Heating the lithium substituted MnO_2 to 350–400 °C results in a partially ordered HEMD-like MnO_2 (LiMD) phase with higher running voltage and superior discharge kinetics. Continued heating of the lithiated manganese dioxide to 450–480 °C under oxygen partial pressure can result in formation of a mixed phase containing both HEMD and a new, ordered MnO_2 phase (OMD). The intimately mixed HEMD/OMD composition has a discharge voltage near 2.9 V with a capacity about 220 mAh g^{-1}. Heating exhaustively lithiated MnO_2 to 350–400 °C results in formation of the partially ordered LiMD MnO_2 phase as with the previous partially lithium substituted MnO_2. Additional heating of the highly lithium substituted MnO_2 to 450–480 °C under oxygen results in formation of the new OMD phase in substantially pure form. Discharge of the new OMD phase shows it has a discharge capacity near 200 mAh g^{-1} between 3.4 and 2.4 V versus lithium in a single, well-defined discharge process. OMD demonstrated good cycling against Li with no indication of formation of $LiMn_2O_4$ spinel after 80 deep discharge cycles.

Keywords: Manganese dioxide; Lithium battery; Ion exchange; Cation vacancy; SPECS; MAS NMR

1. Introduction

Lithium/manganese dioxide batteries are a high energy density, high drain power source used when the need for high power, voltage and calendar life justifies the comparatively high cost of the cell. Initial efforts to use manganese dioxide as the cathode active material in a nonaqueous lithium battery were unsuccessful owing to gassing caused by the high moisture content of commercial γ-phase manganese dioxides. Ikeda et al. found that heating the manganese dioxide above 300 °C to remove moisture produced an electrochemically active form of manganese dioxide with acceptable gassing characteristics [1]. Detailed investigation showed the heat-treated manganese dioxide, known as HEMD, was mainly a disordered pyrolusite material formed by rearrangement of the ramsdellite MnO_2 in the ramsdellite/pyrolusite intergrowth of the parent γ-manganese dioxide [2]. On discharge, pyrolusite is lithiated in an irreversible process followed by insertion of additional lithium in a reversible process [3,4]. XRD, TEM, CBED and Li MAS NMR studies of the electrochemical lithiation of HEMD revealed the initial irreversible process was lithiation of the defect pyrolusite with a lattice rearrangement to recreate a ramsdellite lattice followed by additional lithiation of the ramsdellite [4].

It was found that a more stable cell resulted if the sodium content of manganese dioxide was be replaced by treatment with acid followed by LiOH solution prior to heat treatment [5,6]. Later work showed that exhaustive treatment of the MnO_2 with LiOH solution or mechano-chemical lithiation conditions resulted in more extensive lithium incorporation into the MnO_2 [7]. After heat treatment, a new manganese dioxide phase, referred to as LiMD was formed [8–10].

The process of lithium incorporation into the γ-manganese dioxide has been identified as an ion exchange process in which

* Corresponding author. Tel.: +1 781 292 8530; fax: +1 781 292 8615.
E-mail address: bill_bowden@gillette.com (W. Bowden).

0378-7753/$ – see front matter © 2006 Elsevier B.V. All rights reserved.
doi:10.1016/j.jpowsour.2006.10.041

protons in the surface, vacancy and groutite sites in the MnO_2 are successively replaced by lithium [11]. In this work, the replacement of protons with lithium is shown to have a profound impact on the electrochemical behavior of manganese dioxide and to lead to formation of new manganese dioxide related materials of potential importance as cathode materials in lithium batteries.

2. Experimental

2.1. Preparation of partially lithiated γ-manganese dioxide

In a typical experiment, 800 g electrolytic manganese dioxide (Kerr-McGee Chemical Co.) was dispersed in about 1500 cm^3 distilled water with vigorous stirring and 300 cm^3 3 M sulfuric acid was added. After about 1 h, the stirring was terminated and the MnO_2 allowed to sediment. The supernatant sulfuric acid solution, now containing the ion exchangeable sodium from the MnO_2 was decanted, the MnO_2 washed once with 1500 cm^3 water and then once more dispersed in 1500 cm^3 water. Solid $LiOH{\cdot}H_2O$ was then gradually added to the stirred suspension. With addition of the LiOH, the MnO_2 suspension became a chocolate color as the MnO_2 peptized and became darker as the MnO_2 re-agglomerated. After $LiOH{\cdot}H_2O$ had been added to achieve the target pH, the MnO_2 was allowed to stand overnight. The pH was again measured and minor further additions of $LiOH{\cdot}H_2O$ were made to regain the target pH. The lithiated MnO_2 was isolated by filtration and dried overnight at 110 °C to produce a dark free-flowing powder. The lithiated MnO_2 was then heated in air to 350 °C for 7 h to form LiMD. LiMD synthesized by this procedure varies from 0.38 to 0.95% Li.

2.2. Preparation of mixed HEMD and OMD

The lithiated γ-manganese dioxide described above was placed in a retort furnace provided with a slow bleed of oxygen to blanket the sample and heated to 450 °C for 24 h before being allowed to cool to ambient temperature.

2.3. Preparation of extensively lithiated γ-manganese dioxide

The procedure above was repeated with the key modification that the lithiation was carried out at elevated temperature by heating the $LiOH/MnO_2$ suspension on a hot plate to 60 and 80 °C, respectively. To prepare the most exhaustively lithiated manganese dioxide samples, the suspension was also made 1 M in LiBr to increase the lithium concentration.

2.4. Preparation of $LiMn_4O_8$

The exhaustively lithiated manganese dioxide described above was placed in a retort furnace provided with a slow bleed of oxygen to blanket the sample and heated to 450 °C for 24 h before being allowed to cool to ambient temperature.

Electrochemical results were obtained from 2430 size crimp-sealed coin cells. Cells were modified to assure cathode limited construction. Cathodes were formed by mixing a composition of 60% MnO_2, 30% graphite (KS-6) and 10% Teflon powder in a blender and then by pressing a cathode pellet containing about 300 mg active material into the can.

SPECS discharges were performed with an Arbin multichannel potentiostat at stepping rate of 5 mV each hour and 5 mV every 2 h, while cell discharges were done using a Maccor battery test system.

The X-ray diffraction scans were carried out on a Rigaku Miniflex Diffractometer using Co Kα radiation and a scanning rate of 0.01° (two φ) per second. Results were electronically converted and plotted as Cu Kα radiation. The samples were prepared by packing powders of MnO_2 into aluminum holders covered by a glass slide, producing a dense agglomerate of powder with a macroscopically flat surface suitable for X-ray diffraction studies.

3. Results

3.1. Lithiation of EMD

Li content varies as a function of base and pH. EMD as prepared contains substantial numbers of protons that are evolved as water during heating and drying processes. One popular chemical formulation of EMD defines three proton environments in EMD [12].

1. Physisorbed surface moisture desorbed as water near 110 °C.
2. Protons present in cation vacancies in the Mn (4+) lattice providing charge balance for "missing" Mn (4+) ions.
3. Protons present in groutite (2 × 1) tunnel sites and providing charge balance for Mn (3+) ions in the Mn (4+) lattice.

MAS NMR studies of EMD synthesized in deuterium media have supported Ruetschi's classic work [13,17]. Earlier work showed that LiOH base treatment of EMD resulted in some replacement of protons in both surface and cation vacancy environments by lithium [11,13]. Weight loss studies of typical EMD materials suggest that commercial EMD can be expressed by a rough analysis of $H_{(0.22)}MnO_2$, making the limit for a lithium ion exchanged EMD at about 1.85% lithium. Lithium exchanged EMD samples were dried at 110 C to remove surface moisture and analyzed for lithium with results given in Table 1. As shown in the table, treatment with strong aqueous LiOH results in about 50% replacement of protons by lithium. Increased temperature

Table 1
Lithium content of EMD after ion exchange with lithium

pH	Temp.	% Li
9	20	0.28
10	20	0.38
11	20	0.54
12	20	0.64
13	20	0.86
13 (LiOH/LiBr)	60	1.45
13 (LiOH/LiBr)	80	1.80
13 (LiOH/LiBr)	120	2.25

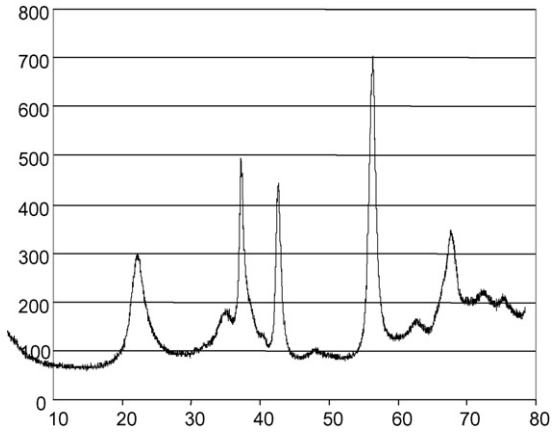

Fig. 1. XRD of lithium exchanged EMD with 1.8 w/o Li in place of protons is superimposable with the XRD pattern of the parent EMD.

and greater mass action by addition of LiBr to the lithiation mix result in high lithium content. Apparently stoichiometric lithium replacement of protons is attained at 80 °C. Hydrothermal lithiation results in even higher lithium contents but the mechanism by which this is achieved is unclear and we suspect there are reduction processes taking place with formal reduction of the manganese oxidation state.

The XRD pattern of the lithium exchanged EMD in Fig. 1 is unchanged from that of the original proton-containing manganese dioxide and indicates the lack of long-range order in both protons and lithium in the MnO_2.

Li MAS NMR of the highly lithiated EMD is shown in Fig. 2. Spinning side band satellite peaks are marked with asterisks. The sharp resonance near 0 ppm and its' side bands are due to diamagnetic lithium. This lithium experiences no chemical shift from the Mn and is presumably lithium in sites on the surface of the manganese dioxide. The broad peak centered about 400 ppm is thought to be due to lithium experiencing some line broadening brought about by the Mn (4+) in the MnO_2 lattice. Model compound studies have show that Li near octahedral Mn (3+) has a resonance near 100 ppm while Li near Mn (4+) has a resonance near 600 ppm [13,14]. We interpret the 400 ppm resonance as indicating lithium in cation vacancy sites experiencing some line broadening due to the nearby Mn (4+) lattice. Lithiated EMD dried at 250 °C still maintains the EMD (γ-MnO_2) structure, as shown by the XRD pattern, but has little or no residual

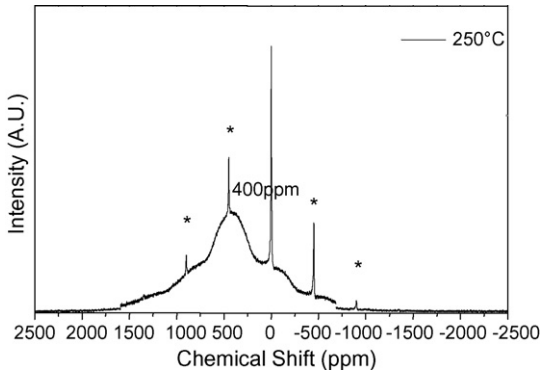

Fig. 2. Li MAS NMR of lithium exchanged EMD with about 1.8 w/o lithium.

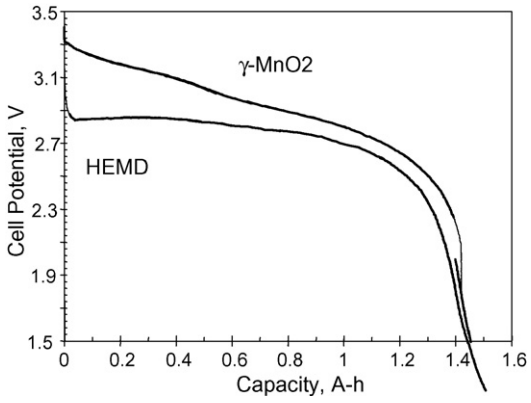

Fig. 3. Comparison of discharge curves of HEMD and lithiated EMD against lithium in 2/3A size cells.

moisture known to cause gassing in primary Li/MnO_2 batteries. The lithiated EMD is electrochemically active in nonaqueous electrolytes and discharges against metallic lithium in a carbonate ester/DME electrolyte with a capacity of 260 mAh g^{-1}. The capacity on a 100 Ohm discharge is comparable to that of a conventional heat treated EMD (HEMD) cathode as shown in Fig. 3. While gravimetric capacity of the lithium exchanged EMD is comparable to HEMD, the running voltage is quite different as indicated in the 2/3A size cells discharged in Fig. 3. In contrast to the reasonably flat HEMD discharge near 2.8 V, the lithiated EMD discharges in a smooth curve from about 3.4 to 2.8 V and has an overall running voltage about 300 mV superior to HEMD.

Stepped Potential Electrochemical Spectroscopy (SPECS) is a useful tool to determine discharge process and reaction mechanism for reduction of an experimental cathode material [15,16]. SPECS discharge at a rate of 5 mV an hour was performed on the lithium exchanged EMD in a lithium coin cell. The plot of capacity for each 5 mV segment of the discharge is shown in Fig. 4 below and indicates there are two discharge processes, one centered at 3.25 V and the other centered about 2.9 V. Examination of the current–time plot from this experiment reveals that both reduction processes in lithium exchanged EMD involve reversible lithium insertion processes, in contrast to the irreversible process seen with HEMD. It is an attractive hypothesis to assign the 3.25 V process to reduction of ramsdellite domains in the EMD while the 2.9 V process is due to reduction of pyrolusite sites in the EMD. The contrast in voltage between the 2.9 V pyrolusite process in EMD and the 2.7 V pyrolusite reduction observed with HEMD is due to the linear nature of the pyrolusite defects in EMD compared to the bulk pyrolusite in HEMD [16].

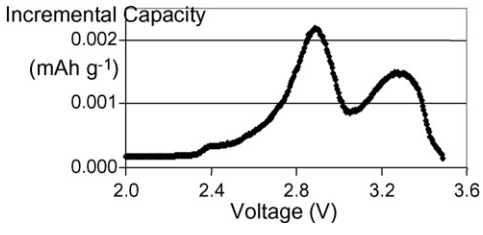

Fig. 4. SPECS differential capacity plot for discharge of lithiated EMD.

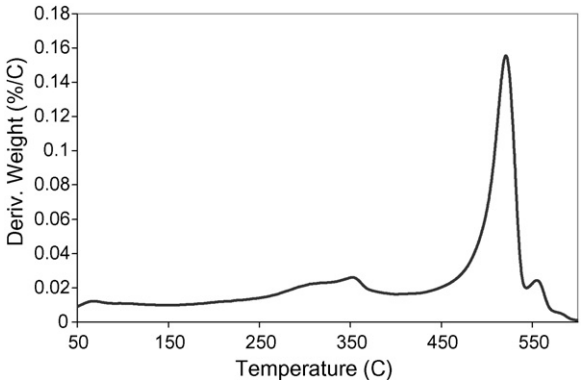

Fig. 5. dTGA curve of EMD showing beta-conversion process near 350 °C followed by formation of Mn_2O_3 near 450 °C.

We suggest the reversible lithiation process indicates better current capability and less polarization during discharge leading to better current capability and higher running voltage for the lithium exchanged EMD.

Weight loss during heating was examined by use of TGA and dTGA plots. Figs. 5 and 6 compare dTGA curves for EMD and lithiated EMD. As shown in Fig. 5, EMD has an initial weight loss process near 100 °C assigned to loss of surface water followed by a second near 350 °C from the loss of vacancy and lattice protons and formation of HEMD and ending with loss of O_2 and formation of Mn_2O_3 near 500 °C. The HEMD formation process involves loss of protons and transformation of ramsdellite domains in the EMD to defect pyrolusite structures. The dTGA plot for lithiated EMD shows processes at the same temperatures and presumably assigned to similar processes as well as a previously unknown process near 450 °C.

Earlier work had shown that partially lithiated EMD underwent a phase change near 350 °C leading to formation of an ordered intergrowth structure [8–10]. The transition near 450 °C was unexpected. XRD of lithiated EMD heated to 450 showed traces of Mn_2O_3 that were eliminated by presence of an oxygen atmosphere so that subsequent experiments adopted the O_2 atmosphere as standard.

The chemistry of moderately lithiated (ca. 0.9% Li) EMD has been discussed previously [9]. The extensively lithiated EMD forms a similar material on heating to 350 °C as shown by the XRD pattern in Fig. 7.

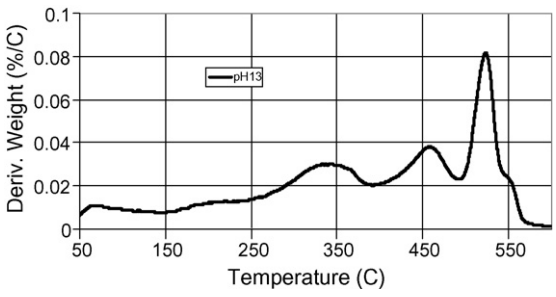

Fig. 6. dTGA curve of lithiated EMD showing formation of two lithiated manganese dioxide phases at 350 and 450 °C before oxygen loss and Mn_2O_3 formation near 480 °C.

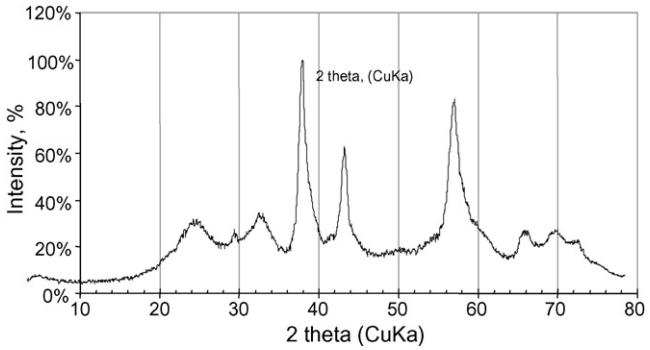

Fig. 7. XRD pattern of extensively lithiated EMD after heat treatment at 350 °C.

Li MAS NMR of the ordered intergrowth structure once more indicates presence of lithium in three environments, namely diamagnetic surface sites near 0 ppm, manganese vacancy sites near 400 ppm and ramsdellite tunnel site s near 590 ppm as shown in Fig. 8 below. Compared to the Li MAS NMR of the 0.9% Li intergrowth, it is possible the 1.8% lithium intergrowth shows presence of comparatively more lithium in ramsdellite tunnel sites. The lithiated intergrowth discharges against lithium in two closely coupled steps with a total capacity of 240 mAh g^{-1} as shown in Fig. 9. A SPECS plot of capacity over 5 mV increments compared to voltage shows discharge processes centered about 3.1 and 2.9 V.

Moderately lithiated (0.9%) EMD undergoes first the transition to the ordered intergrowth at 350 °C then on further heating to 450 °C under oxygen decomposes to an intimate mixture of HEMD (pyrolusite phase) and a new phase as shown in Fig. 10.

Extensively lithiated EMD with about 1.8% Li content forms the new phase in substantially pure form after heating to 450 °C under oxygen as shown in Fig. 11.

As shown above the XRD pattern has some unique features for a ramsdellite/pyrolusite intergrowth material with comparatively sharp peaks and a well-defined peak at 22° and almost complete absence of the normally very strong peak near 57°. We propose this new material is an ordered monoclinic lithiated manganese dioxide in Section 4 below. From the lithium content the new phase has the approximate composition $LiMn_4O_8$. Li MAS NMR of the new material is presented in Fig. 12 below and reveals two characteristic resonances, the 0 ppm resonance assigned to diamagnetic or surface Li and a resonance near 600 ppm assigned to lithium in ramsdellite tunnel sites as shown in Fig. 12. NMR spectra of the monoclinic phase and its' inti-

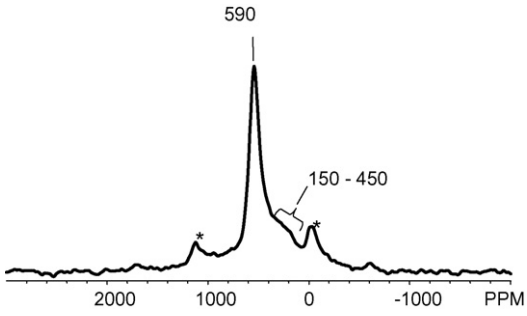

Fig. 8. Li MAS NMR of extensively lithiated EMD after heating at 350 °C.

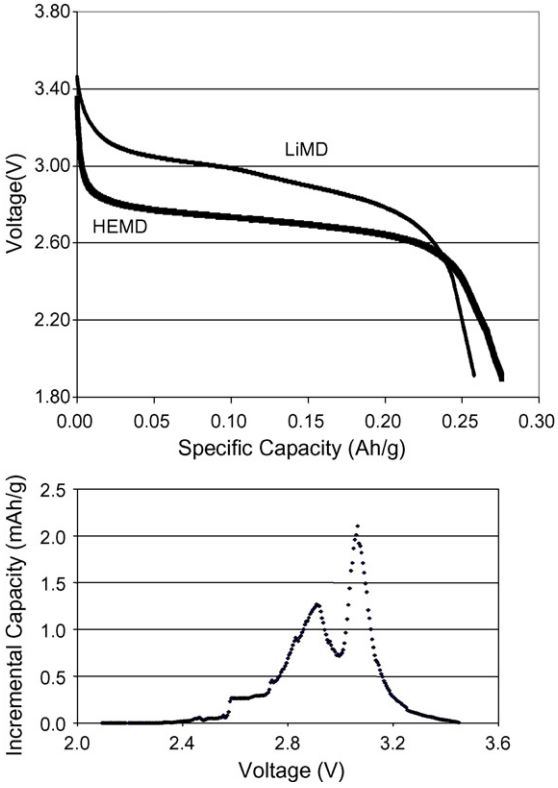

Fig. 9. Top: Plot of voltage vs. capacity for extensively lithiated EMD intergrowth from 350 °C heat treatment. Bottom: SPECS capacity plot shows two discharge processes near 3.1 and 2.9 V.

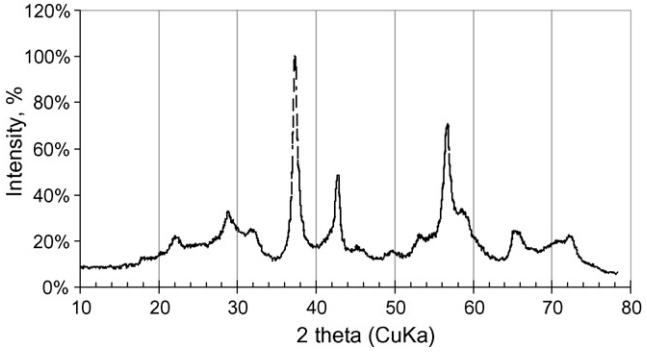

Fig. 10. XRD pattern or moderately lithiated EMD after heating to 450 °C in oxygen atmosphere.

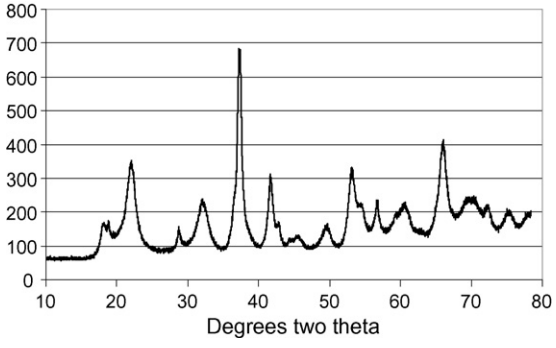

Fig. 11. XRD pattern of the monoclinic phase of extensively lithiated EMD after heating to 450 C under oxygen.

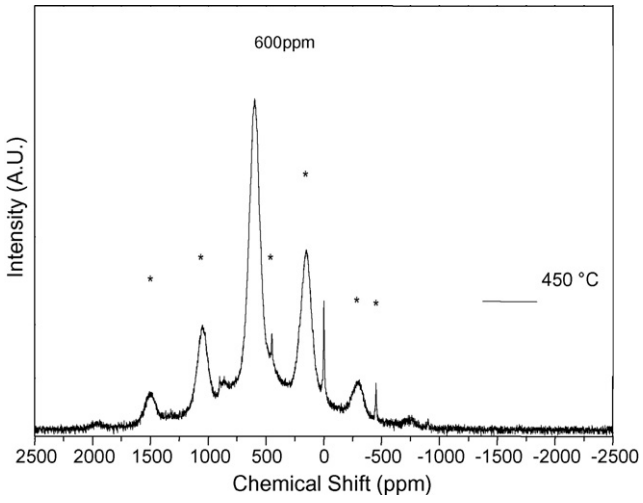

Fig. 12. Li MAS NMR of monoclinic ordered lithiated manganese dioxide.

mately mixture with HEMD are qualitatively identical since the HEMD phase has no lithium content.

Electrochemical properties of monoclinic $LiMn_4O_8$ and its intimate mixture with HEMD were examined by discharge against lithium and use the SPECS discharge method. Discharge of the intimate mix of HEMD and $LiMn_4O_8$ is shown in Fig. 13.

Reduction of $LiMn_4O_8$ shows up as a sharp peak near 2.9 V while reduction of the intimate HEMD mixture appears as a shoulder on the 2.9 V peak closer to 2.8 V. Discharge of $LiMn_4O_8$ alone is shown in Fig. 14 and reveals a smooth single discharge process with a capacity of about mAh g^{-1} centered about 2.9 V.

The comparatively sharp XRD pattern for $LiMn_4O_8$ suggests a more crystalline material than normally observed for lithiated MnO_2. Past efforts to make a rechargeable lithium/manganese dioxide couple have been thwarted by rearrangement of the MnO_2 to $LiMn_2O_4$ spinel, a comparatively low capacity material. Since this rearrangement is thought to take place through various defects in the MnO_2 structure, the comparatively crystalline $LiMn_4O_8$ seemed an attractive candidate for a rechargeable system. Lithium ion cells were prepared with $LiMn_4O_8$ cathodes (the carbon electrode was charged by lithiation against a large lithium electrode which was then used as an internal ref-

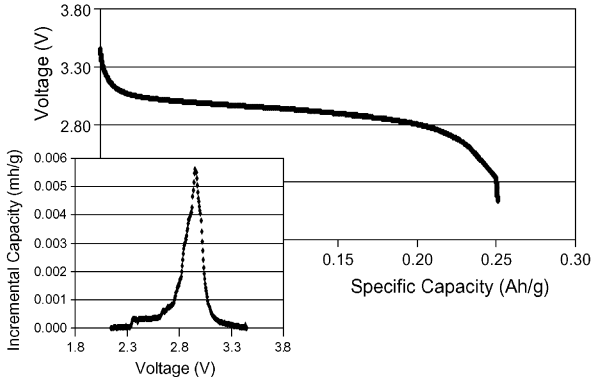

Fig. 13. Discharge of the intimate mixture of $LiMn_4O_8$ and HEMD against lithium with an inset showing presence of two closely coupled discharge processes.

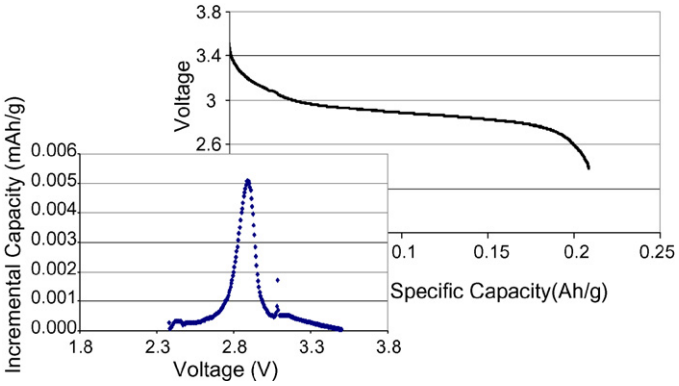

Fig. 14. Discharge of the $LiMn_4O_8$ monoclinic lithiated manganese dioxide.

erence electrode) and discharged and charged at *C*/2 with a 1 h stand in fully charged and discharged state for each cycle. The plot of cell capacity against cycle number is shown in Fig. 15 and indicates reasonably good rechargeability for the $LiMn_4O_8$ while the witness cycle indicates no significant capacity loss during comparatively high rate cycling.

Voltage/capacity plots for cycles 1 and 80 are shown in Fig. 16 and indicate no rearrangement to spinel over the course of the experiment as shown by the absence of the characteristic spinel discharge and recharge voltage plateaus. A witness cycle was performed at low rate after 30 cycles to verify capacity retention and indicated the monoclinic $LiMn_4O_8$ was maintaining a high discharge capacity.

4. Discussion

Treatment of EMD with aqueous lithium hydroxide leads to partial replacement of the proton content of the EMD with lithium ions. Li MAS NMR and chemical analysis show that initially surface protons are replaced by lithium, followed by protons in cation vacancy sites. While chemical analysis suggests that nearly all of the vacancy protons can be replaced by aqueous lithium ions, there was no indication that groutite protons (i.e. in the 2×1 tunnels of the ramsdellite lattice) were replaced in the ion exchange experiment. Guyomard and co-workers recently prepared EMD at relatively high pH in the presence of lithium providing a fascinating opportunity to compare competitive lithium and proton incorporation in EMD during synthesis against the same process as a post-synthesis treatment of the EMD [18].

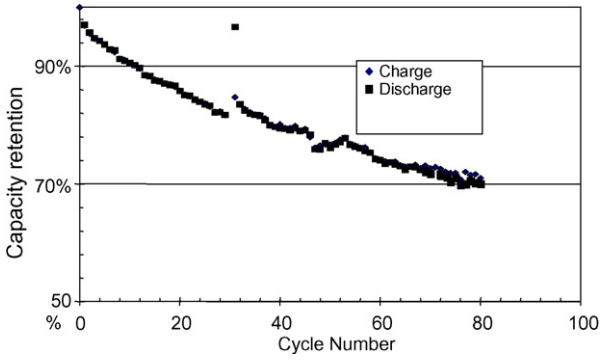

Fig. 15. Plot of capacity against cycle number for $LiMn_4O_8$ cathodes in a lithium ion cell.

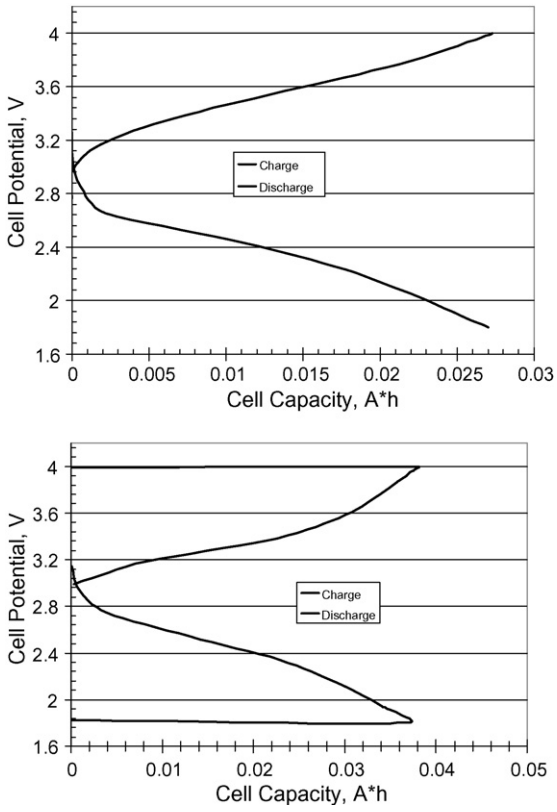

Fig. 16. Voltage/capacity plots for a $LiMn_4O_8$ lithium ion cell showing discharge and charge of cycles 1 (lower) and 80 (upper).

An earlier Li MAS NMR study of partially lithiated EMD showed resonances near 280 ppm while the more or less completely lithiated EMD has a resonance near 400 ppm. We suggest the increased chemical shift in the fully lithiated material is due to sequential replacement of vacancy protons leading to greater lithium–manganese proximity [11].

The ordered intergrowth structure formed near 350 °C has migration of lithium ions from cation vacancy sites into ramsdellite 2×1 tunnels as indicated by the reduction in the broad resonance in the 280–400 ppm area and appearance of a sharper resonance near 570 ppm. It is suggested that the low volatility of lithium oxide compared to water during heat treatment hinders loss of cations from ramsdellite tunnels and enables formation of the more ordered intergrowth structure rather than the thermodynamically stable pyrolusite phase.

Introduction of lithium into ramsdellite tunnel sites forces and increase in the Mn (3+) content of the manganese dioxide and therefore a decrease in the discharge capacity that partially offsets the higher running voltage versus lithium from retention ramsdellite domains in the MnO_2. The gradual decrease of the pyrolusite peak in partly lithiated materials suggests the new phase requires a minimum lithium content. The lower lithium limit for the ordered intergrowth structure is about 0.9% or a composition of about $LiMn_8O_{16}$ while the upper lithium limit was shown to be at least 1.8% lithium or $LiMn_4O_8$.

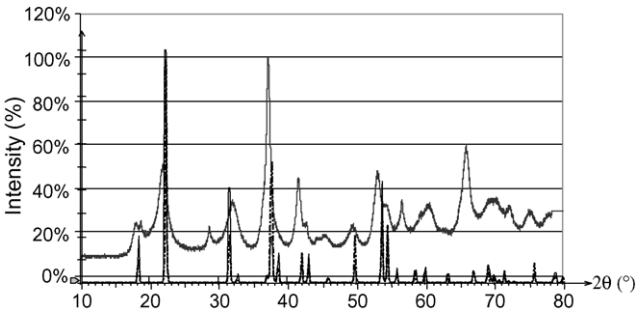

Fig. 17. Comparison of Expected and actual XRD patterns for a monoclinic structure consisting of a 1:1 ratio of ramsdellite and pyrolusite.

The process taking place at 450 °C appears to result in complete movement of lithium from remaining vacancy sites into the 2×1 ramsdellite runnels with a comparatively sharp Li MAS NMR resonance near 600 ppm to form a previously unknown and (for EMD) highly crystalline product. It is suggested this product has a monoclinic unit cell consisting of single ramsdellite and pyrolusite units. Comparison of the expected and actual XRD patterns of the monoclinic $LiMn_4O_8$ is shown in Fig. 17 below. The XRD pattern for this new phase is remarkably similar to that proposed by Verbaere and Hill as "Highly Ordered Manganese Dioxide" (HOMD) and shows clear similarities to structures predicted by Chabre and Pannetier as more ordered pyrolusite–ramsdellite intergrowths [15,19].

The formation of HEMD pyrolusite in the 450 °C heat treatment of lithiated EMD suggests that lithium in the ramsdellite tunnels has only a limited ability to stabilize the ramsdellite lattice against thermal decomposition. At 350 °C a single lithium ion appears adequate to stabilize more than 8 MnO_2 units (recalling that some lithium is still in vacancy sites and in surface sites) while at 450 °C only about 4 MnO_2 units can be maintained.

Comparative cyclic voltammetry study of the lithiated EMD materials compared to HEMD is shown in Fig. 18. As shown in the figure, retention of the comparatively disordered, high surface area EMD structure leads to a significant voltage increase over HEMD. Subsequent heat treatment to produce more ordered phases with reduced surface result in a net loss of both capacity and voltage but the voltage of the more ordered materials remains higher than HEMD due to retention of the ramsdellite structure.

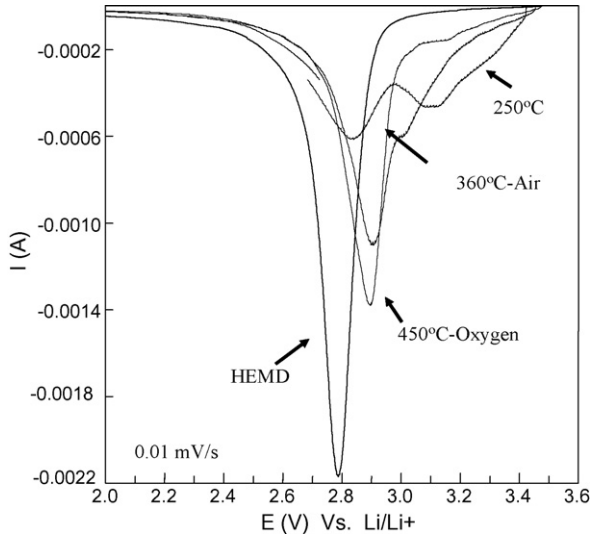

Fig. 18. Comparison of electrochemistry of HEMD, lithiated EMD and intergrowth EMD and monoclinic $LiMn_4O_8$ by CV.

5. Conclusions

It has been shown that lithium-proton exchange in electrolytic manganese dioxide can take place in aqueous media leading to essentially complete replacement of surface and vacancy protons by lithium while groutite (Mn 3+) protons remain substantially unaffected. The resulting lithiated EMD is a useful cathode material in its own right in lithium batteries since it has a higher running voltage and is also a useful intermediate material useful for preparation of lithium containing manganese dioxides where the favorable ramsdellite structure is stabilized to higher temperatures by presence of lithium in the MnO_2 lattice. The most crystalline of the lithiated MnO_2 materials has an approximate composition of $LiMn_4O_8$ and is an interesting rechargeable cathode material for lithium batteries with a capacity around 210 mAh g^{-1} and a running voltage of about 2.9 V.

References

[1] Ikeda, et al., Manganese dioxide as cathodes for lithium batteries, in: Proceedings of the Manganese Dioxide Symposium, vol. 1, Cleveland 1975, U.S. Patent 4,133,856 (1979) (attendees: Ikeda, Hironosuke, Hara, Mitsunori, Narukawa, Satoshi).
[2] Y. Shao-Horn, S.A. Hackney, B.C. Cornilsen, J. Electrochem. Soc. 144 (1997) 3147.
[3] J.C. Nardi, J. Electrochem. Soc. 132 (1985) 1787.
[4] W. Bowden, C. Grey, S. Hackney, X.Q. Yang, Y. Paik, F. Wang, T. Richards, R. Sirotina, ITE Lett. 3 (3) (2002) B1.
[5] W. Bowden, M. Capparella, R. Fooksa, US 5,698,176, December 16, 1997.
[6] M. Capparella, W. Bowden, R. Fooksa, US 5,863,675, January 26, 1999.
[7] P. Christian, O. Mao, US 6,403,257, 2002.
[8] N. Iltchev, P. Christian, W. Bowden, R. Moses, K. Brandt, US Patent 6,190,800 (2001).
[9] N. Iltchev, P. Christian, W. Bowden, P.R. Moses, K. Brandt, ITE Lett. 2 (2001) 349.
[10] Y. Paik, W. Bowden, T. Richards, C. Grey, J. Electrochem. Soc. 152 (2005) A1539.
[11] W. Bowden, C.P. Grey, S. Hackney, F. Wang, Y. Paik, N. Iltchev, R. Sirotina, J. Power Sources 153-2 (2006) 265.
[12] P. Ruetschi, J. Electrochem. Soc. 135 (1988) 2657.
[13] Y. Paik, J. Osegovic, F. Wang, W. Bowden, C. Grey, J. Am. Chem. Soc. 123 (38) (2001) 9367–9377.
[14] Y. Paik, Y. Lee, F. Wang, W. Bowden, C. Grey, Materials Research Society Symposium Proceedings (2001) 658 (Solid-State Chemistry of Inorganic Materials III), GG9.11.1–GG9.11.5.
[15] Y. Chabre, J. Pannetier, Prog. Solid State Chem. 23 (1995) 1–130.
[16] W. Bowden, R. Sirotina, S. Hackney, ITE Lett. 1 (6) (2000) B27.
[17] W. Bowden, C. Grey, S. Hackney, X.Q. Yang, Y. Paik, F. Wang, T. Richards, R. Sirotina, ITE Lett. 3 (3) (2002) B1.
[18] E. Machefaux1, T. Brousse, A. Verbaere, J.L. Duvail, G. Ouvrard, D. Guyomard, IBA-HBC 2006, January, 2006.
[19] L.I. Hill, A. Verbaere, J. Solid State Chem. 177 (12) (2004) 4706–4723.